# A Robust Inter-Connecting Layer for Achieving High Performance Tandem Polymer Solar Cells

*Jun Yang,* Rui Zhu, Ziruo Hong, Youjun He, Ankit Kumar, Yongfang Li, and Yang Yang**

Recently, polymer solar cells (PSCs) have attracted much attention primarily due to their potential for fabricating low-cost and large-area flexible solar cells.[1–3] Smart chemistry can design conjugated polymeric structures for PSCs with enhanced open-circuit voltage ($V_{OC}$) and short-circuit current density ($J_{SC}$). This has resulted in significant efficiency enhancements in recent years. Nonetheless, most of the materials designed today always suffer from the inherent disadvantage of not having a broad absorption range, which limits the utilization of the full solar spectrum.[4,5] A possible solution is to stack multiple photoactive layers wherein the photoactive layers have complementary absorption. Recently, multiple-junction tandem PSCs with various configuration have been demonstrated, in which two polymer:fullerene bulk heterojunctions (BHJs) are connected in series or parallel to fulfill this goal.[6–8] These configurations enable reduction of potential loss during photon-to-electron conversion process, and add-up of electrical potential or photocurrent of the individual BHJs, while the combination of polymers with complimentary bandgaps broadens absorption band ranging 300 nm up to 900 nm, covering a larger portion of the solar spectrum. Recently, a 7.7% PCE from small organic molecule-based tandem solar cells has been achieved.[9] It strongly indicats that tandem structure is one of the promising approaches to break though 10% theoretical limit for single-junction-based polymer solar cells.[10]

In addition to the requirement for photoactive materials, a serial-connected tandem cell requires an inter-connecting layer (ICL) that joins the sequential subcells. It has to satisfy the following requirements. The ICL must ensure resistance-free electrical connection between subcells therefore there is no/minimal electric potential loss. The ICL serves as charge recombination zone aligning the quasi-Fermi level of holes in one subcell to that of electrons in the other, in which charge carriers recombine consequently. Optically, it must be transparent to minimize absorption loss in the ICL. Most importantly, from the point of view of realizing successful tandem cells, the ICL should be physically robust to protect the underlying layers against damage from further solution processing of the rear subcell.

The ICLs consisting of n-type metal oxides combined with high-workfunction metallic poly(3,4-ethylenedioxythiophene):-poly(styrenesulfonate) (PEDOT:PSS) have been used for tandem polymer solar cells.[8,11–13] Commercially available PEDOT:PSS which has been used in these previous reports has good film formation properties, sufficient electrical conductivity and high optical transparency. Unfortunately, processability has become the top critical issue to design and fabricate a successful tandem PSC. The reason is that PEDOT:PSS films have a thickness of only several tens of nanometers, and metal oxide layers are normally amorphous and not dense enough to protect the lower layers (front subcell) when depositing the second subcell (rear cell) by solution process. The penetration of solvents through the ICL may disturb charge carrier selectivity of the ICL between the two subcells, and thus enhance the charge recombination loss. Therefore, reduced $V_{OC}$ has been widely observed from tandem cells using these materials as ICLs.

Currently, fast-drying solution process of the rear subcell (using solvents with low boiling point, such as chloroform or dichloromethane) is being used to partially circumvent this problem.[8,11–13] It has been well understood that for single BHJ PSCs the optimal processing parameters vary significantly with different type of polymers. However, this limits the choice for processing the rear cell, and thus its performance in tandem architectures. Its processing cannot take full advantage of well established processing methods for achieving maximal efficiency, for example, a slow growth solvent annealing approach, addition of high boiling point tertiary solvent, and using a high boiling point solvent in general.[3,14–16] Obviously, the existing ICL materials, in spite of their many features, have fatal flaws to be utilized as a reliable approach for tandem PSC design and efficiency improvement. It is to fulfill this technology gap that we need a multi-functional ICL to sustain the solution deposition of the rear layer.

In this work, a modified PEDOT:PSS (m-PEDOT) layer was developed to be physically robust enough to endure slow drying solvents such as chlorobenzene (CB) and dichlorobenzene (DCB). Furthermore, we are able to modulate the optical field distribution in the devices by varying the thickness of the ICL, as confirmed via optical simulations. This ICL widely broadens the solvent selection for the secondary active layer process and eases the fabrication process of polymer tandem solar cells, so that each subcell is fabricated from its optimal solvent and deposition conditions, enabling us to achieve a high efficiency of 7% for polymer tandem solar cells under AM1.5G spectrum (100 mW/cm$^2$) and 7.8% under lower light intensity (10 mW/cm$^2$). In addition, considering the importance of layer-by-layer solution

J. Yang, Dr. R. Zhu, Dr. Z. Hong, A. Kumar, Prof. Y. Yang
Department of Materials Science and Engineering
University of California Los Angeles
Los Angeles, CA 90095, USA
E-mail: jun.yang@ucla.edu; yangy@ucla.edu
Dr. Y. He, Prof. Y. Li
Beijing National Laboratory for Molecular Science
Institute of Chemistry
Chinese Academy of Sciences
Beijing, 100190, P. R. China

**DOI: 10.1002/adma.201100221**

process for applications in other fields, our ICL could be applied into organic light emitting devices and thin film transistors.

The m-PEDOT solution was made by mixing commercial PEDOT:PSS (PH500, from H. C. Stark) with sodium polystyrene sulfonate (SPS) aqueous solution (100 mg/ml). Varying the PEDOT and SPS volume ratio changes the viscosity of the solution, and thus the thickness of m-PEDOT layer can be easily tuned. The SPS is a fully transparent material throughout visible and near IR range, so it induces no additional optical loss. Electrically, since good conductivity is essential and critical for the ICL, 5% dimethylformamide (DMF) which is commonly used as the conductivity enhancer for PEDOT:PSS was added to the m-PEDOT solution to further enhance the conductivity. (please see Supporting information for details)[17,18] Note here that efficiency overestimation due to lateral conductivity has been ruled out using simple shadow masks upon measurement.

To know the physical robustness of m-PEDOT layer, we test its durability against CB solvent (see Experimental). With such a simple method, CB is used to rinse the film of front subcell unit with the ICL. **Figure 1**a shows the optical microscope image of PEDOT4083 on poly(3-hexylthiophene) (P3HT): [6,6]-phenyl-$C_{71}$-butyric acid methyl ester ($PC_{70}BM$) after CB treatment. As shown by the arrow, the right part of the image was treated by CB. It is clear that the underlying P3HT:$PC_{70}BM$ film was dissolved and destroyed by the solvent. In contrast, Figure 1b demonstrates that the solvent does not affect the P3HT:$PC_{70}BM$ film protected by m-PEDOT at all. Figure 1c shows tapping-mode AFM height image of m-PEDOT on top of P3HT:$PC_{70}BM$ film. The m-PEDOT layer was relatively smooth with surface roughness of 5 nm, providing a good platform for the second subcell deposition.

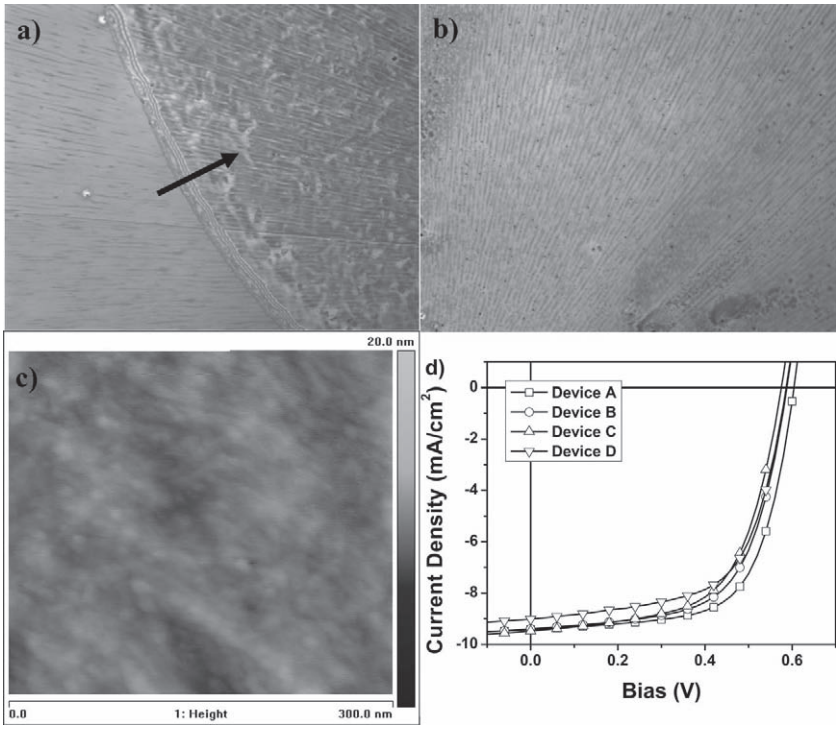


**Figure 1.** Physical property comparison between PEDOT4083 and m-PEDOT. a) Optical microscope image of PEDOT4083 film deposited on P3HT:$PC_{70}BM$ film after CB solvent treatment with a magnification of 40X. b) Optical microscope image of m-PEDOT layer deposited on P3HT:$PC_{70}BM$ film after CB solvent treatment with a magnification of 40X. c) AFM tapping-mode height image of m-PEDOT layer deposited on P3HT:$PC_{70}BM$ film. d) *J–V* characteristic of the devices A-D.

In order to investigate the electrical and physical properties, we construct devices with the following structures, Device A-D:

Device A: ITO/PEDOT/P3HT:$PC_{70}BM$/$TiO_2$/Al

Device B: ITO/PEDOT/P3HT:$PC_{70}BM$/$TiO_2$/PEDOT4083/Al

Device C: ITO/PEDOT/P3HT:$PC_{70}BM$/$TiO_2$/m-PEDOT/Al

Device D: ITO/PEDOT/P3HT:$PC_{70}BM$/$TiO_2$/m-PEDOT (treated by CB)/Al

The current density versus voltage (*J–V*) characteristics of the devices were measured under AM1.5G 100 mW/cm$^2$ illumination as shown in Figure 1d and photovoltaic parameters are listed in supplementary information. The control device (Device A) used $TiO_2$/Al as the cathode. In all the cases, another 0.5 nm of ultrathin aluminum was inserted to improve both the wettability and electrical contact of the $TiO_2$ film on the P3HT:$PC_{70}BM$ layer.[4] An open-circuit voltage ($V_{OC}$) of 0.60 V, a short-circuit current density ($J_{SC}$) of 9.7 mA/cm$^2$, and a fill factor (*FF*) of 65% were obtained, yielding a total efficiency of 3.7%. For Device B and C, additional PEDOT4083 and m-PEDOT layers were inserted between $TiO_2$ and Al cathode, respectively. Both devices had good performance (PCE of 3.4%), showing the good conductivity of the PEDOT layer for charge transport. Device D had the same structure as device C, but before depositing the Al cathode, CB solution was put on top of m-PEDOT layer and then after 30 sec removed by spinning substrate. In order to test the robustness of our ICL, the treatment is even more severe than normal process of the second BHJ from high boiling point solvents. The device still showed reasonable PCE of 3.3% with $V_{OC}$ of 0.59 V, $J_{SC}$ of 9.2 mA/cm$^2$, and *FF* of 61%. However, the device with PEDOT4083 was damaged after CB treatment. The device shorted every time. This confirms that our m-PEDOT layer has enough robustness to protect the underlying polymer film from the high-boiling point, slow drying solvent. To fully prove the feasibility of the ICL, we also construct tandem devices which the second active layers are fabricated from high-boiling point solvent by slow drying methods (please see Supporting information for details). Unprecedentedly, we successfully connected two subcells via solvent annealing process. Normally it takes at least 20 min for DCB solvent to dry in the solvent annealing process. As can be seen clearly, the front subcell was NOT affected, and the $V_{OC}$ add-up of the two subcells is the direct proof of robustness of this convenient ICL.

With that, we explore more functionalities of our ICL. The high transparency and conductivity of the ICL also provide tenability of its thickness over large range from a few tens of

nanometer to several hundred. Considering typical refraction index of 1.5 to 2.0 in organic compounds, the ICL becomes a powerful tool for us to manipulate optical field distribution in multi-layered structures. The ease of optical field tuning in the tandem device by using the m-PEDOT as a spacer layer is shown in Figure SI-2 of the Supporting Information and the relative photon flux absorption profile is shown in **Figure 2**a. The thickness of m-PEDOT is controllable ranging from tens to hundreds of nanometers; by varying the ratio of SPS stock solution to the PH500 and tuning the viscosity of the m-PEDOT solution. The devices of the structure C having various m-PEDOT thickness of 90, 160 and 240 nm showed $J_{SC}$ of 9.7, 9.0 and 8.8 mA/cm$^2$, respectively, as shown in Figure 2b. Though m-PEDOT causes negligible absorption, our simulation results show that it influences the absorption profile in P3HT active layer significantly. Integrating overall absorption under AM1.5G (exciton generation) in the P3HT reference cells with varied m-PEDOT thicknesses of 90 nm, 160 nm and 240 nm gives the relative values of 1.12, 1.03 and 1 respectively. These data are consistent with EQE measurement, and agree well with *J–V* characteristics. Confirmation of these $J_{SC}$ values comes from external quantum efficiency (EQE) measurement (Figure 2b). Thus, a 90 nm m-PEDOT layer was chosen later for our tandem cell fabrication.

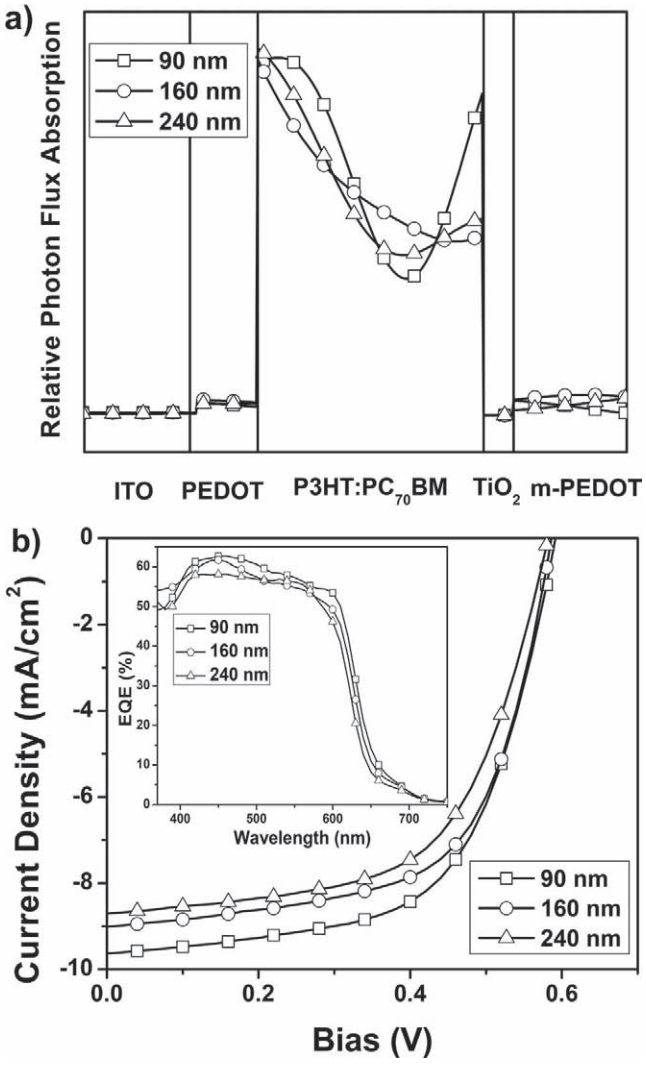


**Figure 2.** m-PEDOT as an optical spacer. a) Calculated relative photon flux absorption of the devices by varying different thickness of m-PEDOT layer with the structure: ITO/PEDOT4083/P3HT:$PC_{70}BM$/$TiO_2$/m-PEDOT/Al. b) *J–V* characteristic and EQE spectra of the corresponding devices in a).

With this versatile and robust m-PEDOT layer in hand, we fabricate highly efficient polymer tandem cells. In our tandem structure, P3HT was used as a front cell and the corresponding acceptor material was indene-$C_{60}$ bisadduct ($IC_{60}BA$).[19] The advantage of this new acceptor is it has similar electric, optical and physical properties compared to commonly used $PC_{60}BM$ or $PC_{70}BM$, but can enhance the $V_{OC}$ of the front cell. The rear cell consists of a lower band gap polymer, poly[(4,4'-bis(2-ethylhexyl) dithieno[3,2-b:2',3'-d]silole)-2,6-diyl-alt-(2,1,3-benzothiadiazole)-4,7-diyl] (PSBTBT), mixed with $PC_{70}BM$. Taking the advantage of rubustness of m-PEDOT film in ICL, CB is used as the solvent to process PSBTBT:PC70BM BHJ, offering superior performance than chloroform in our previous reports.[13,20] Inspite of the myriad choices of high efficiency donor polymers which can be used for the tandem structure, Table SI-1 shows that P3HT and PSBTBT are among the best candidates when complementary absorption and efficiency of the two sub-cells is considered.

Over 300 devices were fabricated based on this ICL with the structure: ITO (150 nm)/PEDOT 4083 (40 nm)/P3HT:$IC_{60}BA$ (150 nm)/$TiO_2$ (20 nm)/m-PEDOT (90 nm)/PSBTBT:$PC_{70}BM$ (100 nm)/Ca (20 nm)/Al (100 nm), and the average PCE was 6.8 ± 0.2% under 100 mW/cm$^2$ illumination of AM1.5G solar simulator. The best performance of the tandem cells was 7.0% with $V_{OC}$ = 1.47 V, $J_{SC}$ = 7.6 mA/cm$^2$, and *FF* = 63% (see **Figure 3**a, and **Table 1**). The EQE of both the single cells and the tandem cell were measured using the published method.[11] Integration of the EQE spectra under the AM1.5G solar spectrum yields $J_{SC}$ values consistent with the one showed in Table 1. To the best of our knowledge, such efficiency is the highest reported data for solution processed polymer-based tandem solar cells. Our structure exhibits significantly enhanced performance under weak light conditions. For one exemplary device, the PCE under 100 mW/cm$^2$ light illumination was 6.6% ($V_{OC}$ = 1.47 V, $J_{SC}$ = 7.5 mA/cm$^2$, and *FF* of 60%), while the PCE increased up to 7.8% at 10 mW/cm$^2$ ($V_{OC}$ = 1.32 V, $J_{SC}$ = 0.88 mA/cm$^2$, and *FF* of 67%). Nearly 20% efficiency gain should be due to the depression of non-geminate recombination in both BHJs, which resulted in higher photorepsonsibility and *FF*. With improved light management using an anti-reflection coating, over 9% PCE of the tandem device is expected under weak light conditions, suggesting potential application for in-door light harvesting.[21,22]

The successful tandem cells allow us to discuss the role and working mechanism of the ICL. Due to the thick m-PEDOT, we are able to sandwiched the ICL between ITO and Al. However, the device is insulating, because both electron and hole injection from conductive m-PEDOT into insulating $TiO_2$ layer is energetic forbidden. After UV illumination, it behaves as a resistor, allowing electron transfer between m-PEDOT and $TiO_2$ no matter forward or reverse bias, while the hole transport should be still blocked by the deep valence band of $TiO_2$. Such

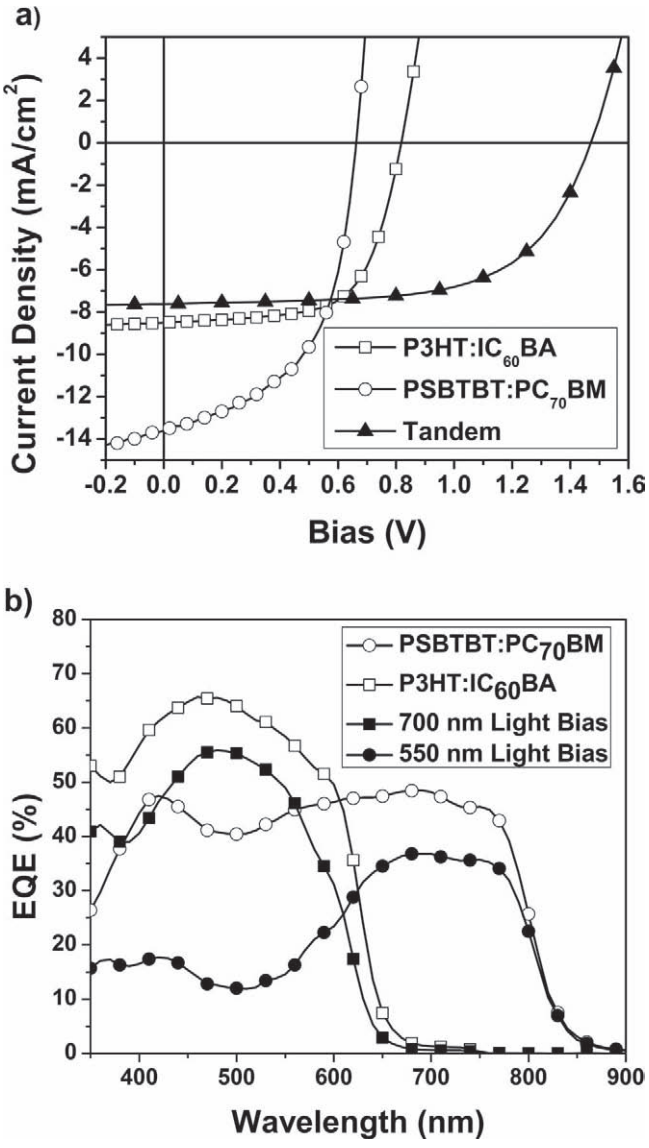


**Figure 3.** Performance of polymer tandem solar cells fabricated based on m-PEDOT. a) *J–V* characteristics of the front and rear reference sub-cells and the tandem solar cell. b) EQE spectra of the front, rear single cells, and tandem solar cell under 700 nm and 550 nm light bias.

light-activation enables good electrical connection for the two subcells. Applying forward bias from ITO side, electron injection from Al may flow through PEDOT/$TiO_2$ interface. Under reverse bias, it is highly possible that both electrons and holes can be injected into the device, and the recombination occurs at the $TiO_2$/PEDOT interface, because PEDOT has higher hole density than electron density in $TiO_2$ films (please see Supporting information for details).

To further scrutinize electrical properties of the ICL in real situation in tandem cells, another device, with Ag inserted at the anode and $V_2O_5$ at the cathode, was constructed, [ITO/Ag (10 nm)/P3HT:$IC_{60}BA$/$TiO_2$/m-PEDOT/PSBTBT:$PC_{70}BM$/$V_2O_5$ (7 nm)/Al]. The corresponding energy diagram is shown in **Figure 4**a. Charge injection is blocked from Ag to P3HT:$IC_{60}BA$ layer due to moderate workfunction of Ag, i.e. 4.3 eV (please see Supporting information for details). Under forward bias, electron injection is blocked form Al to PSBTBT:$PC_{70}BM$ by $V_2O_5$ layer. Under reverse bias, hole injection from $V_2O_5$/Al happens, however, the injected holes should be completely blocked by the $TiO_2$ layer. Therefore, the device should be insulating, as observed from the pristine device. However, after light-activation of $TiO_2$, typical diode behaviors were observed

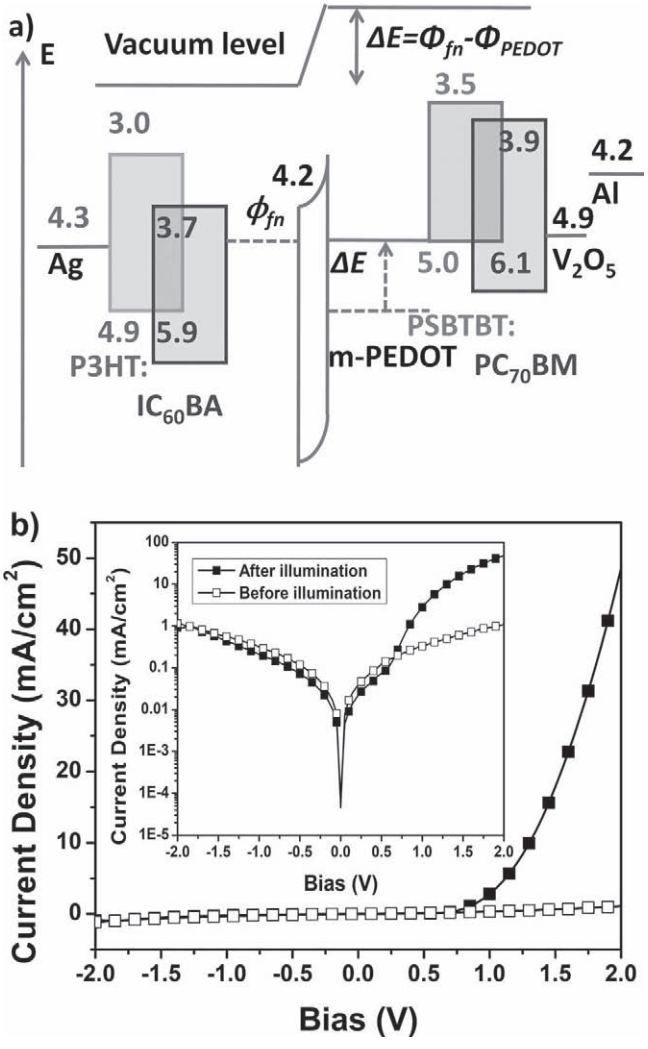


**Figure 4.** Mechanism study of the ICL. a) The energy diagram of the device with the structure: ITO/Ag (10 nm)/P3HT:$IC_{60}BA$/$TiO_2$/m-PEDOT/PSBTBT:$PC_{70}BM$/$V_2O_5$ (7 nm)/Al. b) The dark *J–V* characteristics of the same device in a) before and after light illumination.

**Table 1.** Device performances of the front and rear reference subcells and the tandem solar cells.

| Device | $V_{OC}$ (V) | $J_{SC}$ (mA/cm$^2$) | *FF* (%) | Efficiency (%) |
|---|---|---|---|---|
| P3HT:$IC_{60}BA$ | 0.82 | 8.5 | 65 | 4.5 |
| PSBTBT:$PC_{70}BM$ | 0.66 | 13.7 | 54 | 4.7 |
| Tandem | 1.47 | 7.6 | 63 | 7.0 |

under dark (Figure 4b). This phenomenon strongly suggests charge injection from the ICL into the two subcells, i.e. generation of electrons and holes from the ICL under forward bias and subsequent injection into the front and rear subcells. Taking into account of both electron injection into front subcell and hole injection into rear one, the overall effect of UV activation is to allow electron to flow from the rear subcell into the front one. The UV-activated electrons in $TiO_2$ are hence the origin of the charge generation process, and energy level alignment which enables barrier-free electron injection from m-PEDOT to $TiO_2$, when we combine the two experiments.[23]

In conclusion, we realized a versatile and robust interconnecting layer by which we are able to overcome several critical challenges in polymer tandem solar cells. This layer is ideal in the sense that it is optically transparent to minimize the optical loss, electrically conductive to connect the front and rear cells, physically strong to protect the underlying polymer. With fine optical field tuning by the ICL, preliminary results showed that the PCE of the corresponding tandem cell reaches 7.0% under AM1.5G illumination (with up to 9% with anti-reflection coating under weak light illumination conditions), even higher performance can be expected. Our new ICL offers a general solution to the common challenging issues in the field of solution-processed tandem solar cells, enabling widely broaden the solvent selection for the secondary active layer process and ease the fabrication process of polymer tandem solar cells. Furthermore, considering the importance of layer-by-layer solution process for applications in other fields, our ICL could be generalized to applications for organic light emitting devices and thin film transistors.

## Experimental Section

*Modified PEDOT:PSS (m-PEDOT)*: 400 mg of sodium polystyrene sulfonate (SPS) was weighted and dissolved into 4 ml of deionized water. This stock solution was stirred for overnight and stored under ambient condition for further use. The m-PEDOT solution was made by mixing the commercial available PEDOT:PSS (Clevios PH 500 from H. C. Stark) and SPS stork solution with various volume ratios of 16:1, 8:1, and 4:1, leading the corresponding PEDOT layer 90 nm, 160 nm, and 240 nm, respectively. In order to increase the conductivity of the modified PEDOT, additional 5% DMF was added into the solution and kept stirring for overnight. The m-PEDOT solution is very stable and the performance would not drop even we left it in air for weeks.

*Solvent Test for m-PEDOT to Verify Physical Strength*: To test if m-PEDOT can protect the underlying poly(3-hexylthiophene):[6,6]-phenyl-$C_{71}$-butyric acid methyl ester (P3HT:$PC_{70}$BM) film from the slow drying solvent, we deposited one drop of CB solution on top of PEDOT4083 and on top of a m-PEDOT layer, waited for 30 s, and then quickly removed it by spinning. Other solvents with high boiling point such as DCB also gave the similar results.

*Device Fabrication*: Photovoltaic cells were fabricated on indium tin oxide (ITO) coated glass substrates with a sheet resistance of 15 Ω/square. The PEDOT:PSS (VP AI 4083 from H. C. Stark, PEDOT4083) layer was spin-casted at 4000 rpm for 40 s and annealed at 120 °C for 15 min. The P3HT:H83 at a 1:0.8 weight ratio in 1.8 w.t.% chloroform solution was spin-casted at 4000 rpm for 30 s on top of a layer of PEDOT 4083. After thermal evaporation of 5 Å Al in vacuum, a thin layer of n-type nanocrystalline $TiO_2$ film was spin-casted from 0.2 wt% of $TiO_2$ solution in a 1:1 volume ratio of 2-ethoxyethanol and ethanol at 1000 rpm for 30 s. The films were annealed at 150 °C for 30 min. Then m-PEDOT layer was deposited by spin-coating with 4000 rpm for 40 s. PSBTBT:PC70BM (1:1) from 2 w.t.% chlorobenzene solution was spin-casted and another thermal annealing step was performed at 140 °C for 5 min. The device fabrication was completed by thermal evaporation of 20 nm Ca and 100 nm Al as the cathode under vacuum at a base pressure of $2 \times 10^{-6}$ Torr.

*Electrical, Optical and Microscopic Characterization of Photovoltaic Cells and Thin Films*: The n and k values for the different layers in the tandem cell were measured using an ellipsometer and the values obtained were fed into the software to get the optical field profile. *J–V* characteristics of photovoltaic cells were taken using a Keithley 4200 source unit under a simulated AM1.5G spectrum with an Oriel 9600 solar simulator. Atomic force microscopy (AFM) images were taken on a digital instruments multimode scanning probe microscope.

## Supporting Information

Supporting Information is available from the Wiley Online Library or from the author.

## Acknowledgements

J.Y. and R.Z. contributed equally to this work. Authors are grateful to Dr. L. Huo of UCLA for supplying PSBTBT, G. Yang, L. M. Chen, R. M. Green, S. Sista, and M.-H. Park for helpful discussion and suggestions. This work was financially supported by the AFOSR (Grant No. FA9550–07-1–0264), ONR (Grant No. N000141110250), National Science Foundation (Grant No. CHE0822573), NSFC (Grant No. 50633050, and No. 20821120293), and Solarmer Energy Inc. (Grant No. 20061880).

Received: January 19, 2011
Revised: April 12, 2011
Published online:

[1] N. S. Sariciftci, L. Smilowitz, A. J. Heeger, F. Wudl, *Science* **1992**, *258*, 1474.
[2] S. E. Shaheen, R. Radspinner, N. Peyghambarian, G. E. Jabbour, *Appl. Phys. Lett.* **2001**, *79*, 2996.
[3] G. Li, V. Shrotriya, J. S. Huang, Y. Yao, T. Moriarty, K. Emery, Y. Yang, *Nat. Mater.* **2005**, *4*, 864.
[4] I. Riedel, V. Dyakonov, *Phys. Status Solidi A* **2004**, *201*, 1332.
[5] A. Hadipour, B. de Boer, P. W. M. Blom, *Adv. Funct. Mater.* **2008**, *18*, 169.
[6] J. Gilot, M. M. Wienk, R. A. J. Janssen, *Appl. Phys. Lett.* **2007**, *90*, 143512.
[7] A. Hadipour, B. de Boer, P. W. M. Blom, *J. Appl. Phys.* **2007**, *102*, 074506.
[8] S. Sista, Z. R. Hong, M. H. Park, Z. Xu, Y. Yang, *Adv. Mater.* **2010**, *22*, E77.
[9] C. L. Uhrich, G. Schwartz, B. Maennig, W. M. Gnehr, S. Sonntag, O. Erfurth, E. Wollrab, K. Walzer, J. Foerster, A. Weiss, O. Tsaryova, K. Leo, M. K. Riede, M. Pfeiffer, *Proc. SPIE – Int. Soc. Opt. Eng.* **2010**, *7722*, 77220G.
[10] M. C. Scharber, D. Wuhlbacher, M. Koppe, P. Denk, C. Waldauf, A. J. Heeger, C. L. Brabec, *Adv. Mater.* **2006**, *18*, 789.
[11] J. Y. Kim, K. Lee, N. E. Coates, D. Moses, T. Q. Nguyen, M. Dante, A. J. Heeger, *Science* **2007**, *317*, 222.
[12] J. Gilot, M. M. Wienk, R. A. J. Janssen, *Adv. Mater.* **2010**, *22*, E67.
[13] S. Sista, M. H. Park, Z. R. Hong, Y. Wu, J. H. Hou, W. L. Kwan, G. Li, Y. Yang, *Adv. Mater.* **2010**, *22*, 380.
[14] J. Peet, J. Y. Kim, N. E. Coates, W. L. Ma, D. Moses, A. J. Heeger, G. C. Bazan, *Nat. Mater.* **2007**, *6*, 497.

[15] H. Y. Chen, J. H. Hou, S. Q. Zhang, Y. Y. Liang, G. W. Yang, Y. Yang, L. P. Yu, Y. Wu, G. Li, *Nat. Photonics* **2009**, *3*, 649.
[16] L. M. Chen, Z. R. Hong, G. Li, Y. Yang, *Adv. Mater.* **2009**, *21*, 1434.
[17] J. Y. Kim, J. H. Jung, D. E. Lee, J. Joo, *Synth. Met.* **2002**, *126*, 311.
[18] J. Ouyang, Q. F. Xu, C. W. Chu, Y. Yang, G. Li, J. Shinar, *Polymer* **2004**, *45*, 8443.
[19] Y. J. He, H. Y. Chen, J. H. Hou, Y. F. Li, *J. Am. Chem. Soc.* **2010**, *132*, 1377.
[20] J. H. Hou, H. Y. Chen, S. Q. Zhang, R. I. Chen, Y. Yang, Y. Wu, G. Li, *J. Am. Chem. Soc.* **2008**, *130*, 16144.
[21] L. Schirone, G. Sotgiu, F. P. Califano, *Thin Solid Films* **1997**, *297*, 296.
[22] M. Cid, N. Stem, C. Brunetti, A. F. Beloto, C. A. S. Ramos, *Surf. Coat. Technol.* **1998**, *106*, 117.
[23] M. Terai, T. Tsutsui, *Appl. Phys. Lett.* **2007**, *90*, 083502.